The respiratory complexes I from the mitochondria of two Pichia species

Hannah R Bridges, Ljuban Grgic, Michael E Harbour, Judy Hirst

Biochemical Journal Immediate Publication. Published on 22 May 2009 as manuscript BJ20090492

The respiratory complexes I from the mitochondria of two *Pichia* species

Hannah R. Bridges, Ljuban Grgic, Michael E. Harbour, and Judy Hirst*

The Medical Research Council Mitochondrial Biology Unit, Wellcome Trust / MRC Building, Hills Road, Cambridge, CB2 0XY, U. K.

*Author to whom correspondence should be addressed:
Medical Research Council Mitochondrial Biology Unit, Wellcome Trust / MRC Building, Hills Road, Cambridge, CB2 0XY, U. K.
Tel : +44 1223 252810, Fax : +44 1223 252815, E-mail : jh@mrc-mbu.cam.ac.uk

Page heading title: The complexes I from *Pichia* species

Keywords:
NADH:ubiquinone oxidoreductase
Complex I
Pichia pastoris
Pichia angusta
Electron transport chain
Mitochondria

Abbreviations:
ACMA, 9-amino-6-chloro-2-methoxyacridine;
DDM, n-dodecyl-β-D-maltopyranoside;
DQ, decylubiquinone;
FCCP, carbonylcyanide-p-trifluoromethoxyphenylhydrazone;
FeCN, hexacyanoferrate (III);
FeS cluster, iron-sulfur cluster;
FMN, flavin mononucleotide;
HAR, hexaammineruthenium (III);
dNADH, reduced nicotinamide hypoxanthine dinucleotide (deamino-NADH);
RCR, respiratory control ratio;
ROS, reactive oxygen species.

Synopsis

NADH:ubiquinone oxidoreductase (complex I) is an entry point for electrons into the respiratory chain in many eukaryotes. It couples NADH oxidation and ubiquinone reduction to proton translocation across the mitochondrial inner membrane. Because complex I deficiencies occur in a wide range of neuromuscular diseases, including Parkinson's disease, there is a clear need for model eukaryotic systems to facilitate structural, functional and mutational studies. Here, we describe the purification and characterization of the complexes I from two yeast species, *Pichia pastoris* and *Pichia angusta*. They are obligate aerobes which grow to very high cell densities on simple media, as yeast-like, spheroidal cells. Both *Pichia* enzymes catalyze inhibitor-sensitive NADH:ubiquinone oxidoreduction, display EPR spectra which match closely to those from other eukaryotic complexes I, and show patterns characteristic of complex I in SDS-PAGE analysis. Mass spectrometry was used to identify several canonical complex I subunits. Purified *P. pastoris* complex I has a particularly high specific activity, and incorporating it into liposomes demonstrates that NADH oxidation is coupled to the generation of a proton motive force. Interestingly, the rate of NADH-induced superoxide production by the *Pichia* enzymes is more than twice as fast as that of the *Bos taurus* enzyme. Our results both resolve previous disagreement about whether *Pichia* species encode complex I, furthering understanding of the evolution of complex I within dikarya, and they provide two new, robust and highly active model systems for study of the structure and catalytic mechanism of eukaryotic complexes I.

Introduction

In mitochondria, NADH:ubiquinone oxidoreductase (complex I) catalyses the oxidation of NADH and the reduction of ubiquinone, coupled to the translocation of four protons across the mitochondrial inner membrane, contributing to the proton motive force [1,2]. Fourteen 'core subunits' are conserved throughout the complex I family. They comprise seven membrane bound subunits, encoded by the mitochondrial genome in eukaryotes, and seven hydrophilic subunits, encoded in the nucleus, which form a domain extending into the mitochondrial matrix. The hydrophilic subunits bind a flavin mononucleotide (FMN), at the active site for NADH oxidation, and eight iron sulfur (FeS) clusters. The structure of the hydrophilic domain from *Thermus thermophilus* complex I shows how the FeS clusters enable electron transfer from the flavin toward the quinone binding site [3]. In addition, eukaryotic complexes I contain a variable number of 'supernumerary' subunits. Complex I from *Bos taurus* heart mitochondria has been characterized extensively and contains a total of 45 different subunits [4]. In two fungal model systems, 40 different subunits have been identified in complex I from *Yarrowia lipolytica* [5], and 39 in the enzyme from *Neurospora crassa* [6]. Gabaldon and coworkers have used genomic data to propose how the subunit composition of eukaryotic complex I has evolved [7]; mammalian and fungal complexes I have 21 supernumerary subunits in common, while mammals have ten additional subunits, fungi have three. Mutations in both the nuclearly- and mitochondrially-encoded subunits contribute to the increasing number of complex I deficiencies which have been identified in a wide range of neuromuscular diseases, including Leigh syndrome, leukodystrophy, and Parkinson's disease [8,9].

Studies of eukaryotic complex I rely on model systems to provide sufficient quantities of the enzyme for investigation of its structure and mechanism, and to provide insights into the dysfunction of the human enzyme. The *B. taurus* enzyme is highly homologous to the human enzyme [4], and has proved invaluable in the elucidation of its protein composition, as well as for spectroscopic and functional studies. However, lack of control over the source material, and the impracticality of genetic manipulation, are significant limitations. The intensively studied yeast, *Saccharomyces cerevisiae*, does not encode complex I, but *N. crassa* [10], and more recently *Y. lipolytica* [11], have provided two genetically manipulable fungal enzymes for study.

Figure 1 shows a phylogenetic tree for the dikarya (adapted from [12]), showing that *N. crassa* belongs to the pezizomycotina, and *Y. lipolytica* to the saccharomycetes. *Y. lipolytica* diverged relatively early in evolution from the saccharomyceteceae, which include *Saccharomyces, Kluveromyces, Candida* and *Pichia*. Some of the saccharomycetaceae have lost the complex I genes during evolution, and, in fact, no complex I has been isolated from any of them. Thus, although the *Pichia* genus shows many promising characteristics for the development of a complex I model system (see below), it has not been clear, until now, whether *Pichia* species even express complex I. Sequences for some of the subunits of complex I which are encoded in the mitochondrial genome (known as the ND subunits) have been detected in several species, including *P. pastoris* [13], but attempts to identify an NADH dehydrogenase from *P. pastoris* which is inhibited by a canonical complex I inhibitor, rotenone, were unsuccessful [14]

The two species of yeast described here are *Pichia pastoris* and *Pichia angusta* (previously named *Hansenula polymorpha*). They are both methylotrophic ascomycetes, able to catabolize methanol as their sole carbon source. They are obligate aerobes, and grow on inexpensive, simple media to very high cell densities, particularly in batch-fed conditions. Notably, *Pichia* species grow almost exclusively as yeast-like, spheroidal cells, whereas *N. crassa* grows as filaments, and *Y. lipolytica*

switches between yeast and filamentous growth in response to various environmental stresses [15], a transition known to affect cellular metabolism and protein expression [16]. Both species can be used for overexpression, commonly controlled by the promoter for alcohol oxidase, and induced with methanol [17]. In addition, *P. angusta* can grow at temperatures as high as ~50 °C [18], and therefore may express more stable proteins as part of its heat tolerance. Here, we describe the purification and characterization of the complexes I from *P. pastoris* and *P. angusta*, discuss their suitability as eukaryotic model systems, and compare their properties to those of other members of the complex I family.

Experimental Methods

All chemicals were from Sigma Aldrich or BDH (unless otherwise stated), and chromatographic media were from GE Healthcare. Buffer pH values are reported at room temperature.

Yeast strains and growth

Haploid *P. pastoris* strain X33 (Invitrogen) was grown at 30 °C in 1% yeast extract (ForMedium), 2% peptone (ForMedium) and 2% glycerol (VWR International), initially at pH 5. 60 L of media, in a 70 L Applikon ADI 1075 fermentor stirred at 500 rpm, maintained at 80% pO_2, was inoculated with 2 L of culture, and cells grown until early stationary phase (approx. 24 hours). *P. angusta* strain A-16 (NCYC 2310), a haploid leucine auxotroph of CBS4732, was from The National Collection of Yeast Cultures (UK). Cells were grown at 40 °C in 800 mL aliquots in 2 L flasks (shaken at 250 rpm) until mid stationary phase (approx. 48 hours) in 1% yeast extract, 2% peptone, and 4% glucose, initially at pH 5. *Y. lipolytica* strain GB10 was provided by Prof. U. Brandt (Frankfurt). It was grown at 27 ºC in 2% yeast extract, 4% peptone, and 4% glucose, initially at pH 5.5, in the 70 L fermentor stirred at 500 rpm, maintained at 2% pO_2 (once this value was reached), until late exponential phase (approx. 20 hours). All cells were harvested by centrifugation (5,000 g for 15 min.), then twice resuspended in MilliQ water and recentrifuged. If necessary, cell pellets were frozen at -80 °C. The yields were approximately 41, 27 and 29 g of wet cells per liter of medium for *P. pastoris*, *P. angusta*, and *Y. lipolytica*, respectively. All subsequent steps were at 4 °C.

Isolation of mitochondrial membranes

Methods for cell disruption and membrane isolation were based on those described for *Y. lipolytica* [19,20]. Cells were resuspended to 500 g L^{-1}, in 20 mM MOPS pH 7.2, 400 mM sorbitol (NBS Biologicals Ltd), 0.2% BSA, 5 mM EDTA, 1 mM benzamidine, and 1 mM ε-caproic acid. 1 mM phenylmethanesulfonylfluoride (PMSF) was added immediately prior to cell disruption in a DYNO®-MILL bead mill (Willy A. Bachofen UK Ltd.) maintained below 10 °C (two passes at 10 mL min^{-1}). Cell debris was removed by centrifugation (5,000 g for 15 min.), then the membranes were collected by centrifugation (one hour at 100,000 g (*P. pastoris* and *Y. lipolytica*) or 30,000 g (*P. angusta*)), rehomogenized in 20 mM MOPS pH 7.2, 5 mM EDTA, 1 mM benzamidine, and 1 mM ε-caproic acid, and recollected by recentrifugation. If necessary, membrane pellets were frozen at -80 °C.

Complex I purification

Mitochondrial membranes were homogenized in 20 mM sodium citrate pH 6.5, to 20 mg protein mL^{-1}, and solubilized for 45 min. by the addition of dodecyl-β-d-maltoside (DDM, Glycon GmbH) to 2.3% (*P. pastoris*) or 2.9% (*P. angusta*). Following centrifugation (120,000 g for 45 min.), the supernatant was passed through a MacroCap SP cation exchange column, and dialyzed against 20 mM Tris-Cl pH

7.5 for at least 3 hours. Then, it was loaded onto a Q Sepharose High Performance anion exchange column, pre-equilibrated in 20 mM Tris-Cl (pH 7.5) and 0.15% DDM, and eluted at 2 mL min^{-1}. First, 0.27 M NaCl (*P. pastoris*) or 0.22 M NaCl (*P. angusta*) was applied until the 280 and 420 nm absorbancies became negligible, then complex I was eluted in a sharp gradient to 0.33 NaCl (*P. pastoris*) or 0.27 M NaCl (*P. angusta*), and confirmed using its dNADH:hexaammineruthenium (III) (HAR) oxidoreductase activity. Pooled fractions were concentrated (100 kDa cut-off Vivaspin centrifugal concentrators, Sartorius AG), then injected onto a Superose 6 size exclusion column (0.24 mL min^{-1}, in 20 mM MOPS pH 7.5, 0.05% DDM and 150 mM NaCl). Monomeric complex I eluted from 11 to 14 mL. If necessary, these complex I containing fractions were pooled, concentrated, and reapplied to the column, providing a single, sharp peak. Complex I from *Y. lipolytica* was isolated as described previously, by affinity purification on a Ni-NTA column using a hexahistidine tag on the C-terminus of the NUGM subunit [20,21], followed by size exclusion chromatography on a Superose 6 column *B. taurus* complex I was prepared as described previously [22].

Kinetic measurements

Kinetic measurements were carried out at 32 °C, either in 1 mL cuvettes (Ocean Optics diode array spectrometer), or in 200 µL wells (Molecular Devices microtiter plate reader). Deamino-NADH (dNADH) and NADH were added to 100 µM for ferricyanide (hexacyanoferrate (III), FeCN), HAR and decylubiquinone (DQ) measurements, and HAR, FeCN and DQ to 3.5 mM, 2 mM and 100 µM, respectively. For measurements using DQ, soybean asolectin was added to 0.35 mg mL^{-1} from a 10 mg mL^{-1} stock solution in 20 mM Tris-HCl pH 7.5 and 1% w/v CHAPS (3-[(3-cholamidopropyl)dimethyl-ammonio]-1-propane-sulfonate), Anatrace). Rotenone or piericidin A were added to 5 or 2 µM, respectively, from ethanolic stock solutions. Initial rates of NADH oxidation ($\varepsilon_{340–380\ nm}$ = 4.81 mM^{-1} cm^{-1}) were obtained using linear regression. H_2O_2 and superoxide production were measured at pH 7.5, using 30 µM NADH and either 10 µM Amplex Red and 2 U mL^{-1} horse radish peroxidase (Invitrogen) or 50 µM acetylated cytochrome *c*, as described previously [23].

To produce proteoliposomes containing complex I, 440 µL of 10 mg mL^{-1} soy asolectin (Avanti Polar Lipids Inc.) in 20 mM potassium 3-(N-morpholino) propanesulfonic acid at pH 7.5 (K-MOPS) was homogenised with 60 µL of 10% octyl glucoside. 50 µL of 2 mg mL^{-1} complex I was added, then the detergent was removed by three successive additions of 50 mg Amberlite XAD 2 biobeads (Supelpak) at 1 hour intervals. The proteoliposomes were separated from the biobeads using a syringe fitted with a filter, collected by centrifugation (1 hour at 90,000 g in a Beckman-Coulter MLA 130 rotor), then resuspended in 100 µL K-MOPS. Respiratory control ratios (RCRs) were calculated from the rate of NADH:DQ oxidoreduction, measured (as described above) in the presence and absence of 7 µg mL^{-1} gramicidin (RCR = uncoupled rate / coupled rate). The quenching of the 9-amino-6-chloro-2-methoxyacridine (ACMA) fluorescence at 475 nm was measured using an excitation wavelength of 430 nm, in the presence of 500 nM ACMA and 5 µM valinomycin. Typically, 20 µL of resuspended proteoliposomes were added to 2 mL of assay buffer. When required carbonylcyanide-p-trifluoromethoxy-phenylhydrazone (8 µM, FCCP) or piericidin A (2 µM) were added.

EPR spectroscopy

EPR samples (~15 mg mL^{-1}) were reduced anaerobically with 5 mM NADH, and frozen immediately. Spectra were recorded on a Bruker EMX X-band spectrometer using an ER 4119HS cavity, maintained at low temperature by an ESR900 continuous-flow liquid helium cryostat (Oxford Instruments); the sample temperature was measured with a calibrated Cernox resistor (Lake Shore Cryotronics Inc.).

Analytical methods

Protein concentrations were measured using the Pierce bicinchoninic acid assay. FMN concentrations were analyzed fluorometrically using the method of Burch [24], modified for the plate reader. Iron concentrations were determined using ferene (5,5'(3-(2-pyridyl)-1,2,4-triazine-5,6 diyl)-bis-2-furansulfonate), by the method of Pieroni et al. [25] (except the protein was denatured in 1% HCl and 1.5% trichloroacetic acid, the reducing agent was 0.5% hydroxylamine, and 5 mM thiosemicarbazide was added to bind any copper present).

Protein analyses

SDS-PAGE was carried out on an 18-22% acrylamide gradient, and gels were stained with 0.2% Coomassie Blue R250. Peptide mass fingerprinting and tandem MS were carried out using an Applied Biosystems / MDS SCIEX model 4800 Plus MALDI TOF / TOF mass spectrometer. Database matches to peptide mass fingerprinting and tandem MS data were identified using Mascot (Matrix Science) [26]. Sequences for proposed subunits of *P. angusta* complex I were identified by performing tblastn searches to compare known *Y. lipolytica* and *N. crassa* sequences with the genome survey sequence information from *P. angusta* which is available on the NCBI website.

Results

The presence of both complex I and alternative NADH dehydrogenases in *Pichia* species

Alternative NADH dehydrogenases are single subunit, non-energy transducing NADH:ubiquinone oxidoreductases which are found in many aerobically respiring organisms, either alongside complex I, or, in cases such as *S. cerevisiae*, as a replacement for it (see Figure 1) [27,28]. Alternative NADH dehydrogenases complicate the identification, analysis, and purification of complex I, because the catalytic properties of the two enzymes overlap. Table 1 presents the catalytic properties of mitochondrial membranes prepared from *P. pastoris* and *P. angusta*; in both cases approximately 90% of the NADH binding sites were accessible to the NADH, FeCN and HAR reactants. Three different electron acceptors were used: FeCN and HAR are considered to react at, or close to, the flavin site in complex I, so, unlike DQ, an analogue of the physiological ubiquinone, they do not rely on the functional integrity of the quinone binding site or the membrane domain. First, based on a study of the NADH:ubiquinone oxidoreductases in *E. coli*, dNADH is assumed to react only with complex I [29], so comparing the rates of NADH and dNADH:DQ oxidoreduction by the *P. pastoris* membranes suggests that ~80% of the NADH:DQ oxidoreductase activity is due to complex I. In contrast, for *P. angusta* the rate with dNADH is only ~10% of that with NADH, indicating that one or more alternative NADH dehydrogenases contribute significantly. There is little difference, in either case, between the rates of dNADH and NADH:HAR oxidoreduction, consistent with previous suggestions that HAR does not react with the alternative enzymes [11]. dNADH:FeCN oxidoreduction is significantly faster than dNADH:HAR oxidoreduction in both species, suggesting that FeCN reduction by the *Pichia* complexes I is much faster than HAR reduction. Furthermore, additional FeCN reductases may be present, as suggested by comparison of the dNADH and NADH:FeCN oxidoreductase activities. Note that the concentrations of FeCN and HAR used were chosen because they give close to maximal rates for complex I from *B. taurus*; an extensive investigation of the kinetics of the two *Pichia* enzymes has not been undertaken so far. Second, NADH:DQ and dNADH:DQ oxidoreduction by the *P. pastoris* membranes is 85 and 90% sensitive to the complex I inhibitor piericidin A, consistent with the results described above; the weaker inhibition from rotenone suggests that it is a relatively poor inhibitor in this case. NADH:DQ oxidoreduction by *P. angusta* is not inhibited strongly by either compound,

although, as expected, the dNADH:DQ activity is more strongly inhibited. Taken together, the results in Table 1 indicate that only 10-20% of the NADH:DQ oxidoreductase activity from the *P. angusta* membranes is due to complex I. Interestingly, dNADH:HAR oxidoreduction by the *P. angusta* membranes was optimised by harvesting the cells during stationary phase, and by growing them under high aeration. Similar observations were made previously for *P. jadinii* (also known as *Torulopsis utilis* or *Candida utilis*) [30,31] and *N. crassa* [32]. In particular, mitochondria from *P. jadinii* cells harvested in stationary phase displayed piericidin A sensitive NADH oxidation and the complex I EPR signals N1b and N2, but mitochondria from cells harvested in exponential phase did not.

Purification and confirmation of the complexes I from *P. pastoris* and *P. angusta*

dNADH:HAR oxidoreductase activities were relied upon to guide the development of purification protocols for the two complexes I (see Figure 2). Methods for isolating the complexes I were based on the established protocol for *B. taurus* complex I: solubilization with DDM, anion exchange chromatography, and size exclusion chromatography [22]. Passing the solubilized membranes through a MacroCap cation exchange column, prior to application to the anion exchange column, improved the efficiency of the anion exchange step, particularly for *P. angusta*. For *P. pastoris*, dNADH:HAR oxidoreduction was observed in only one of the major peaks eluting from the anion exchange column (270 - 300 mM NaCl). For *P. angusta*, dNADH:HAR oxidoreductase activity eluted in two major peaks, at 50 to 120 mM NaCl, and 220 to 270 mM NaCl. Only the latter peak catalyzed dNADH:DQ oxidoreduction, and the results below confirm it was complex I. Typically, 1 g of wet cells yielded 12.7 μg of *P. pastoris* complex I, or 7.6 μg of *P. angusta* complex I. In comparison, *Y. lipolytica* has been reported to yield ~30 μg per gram of wet cells by conventional methods [33] or 50 - 100 μg by affinity chromatography [20].

During analytical size exclusion chromatography both *Pichia* complexes I eluted as single, symmetrical peaks at 11.9 ± 0.2 mL (*P. pastoris*) or 12.1 ± 0.1 mL (*P. angusta*). The well characterized complexes from *B. taurus* and *Y. lipolytica* eluted at 11.8 and 11.9 mL, respectively. Their protein molecular masses of ~980 kDa [34] and ~940 kDa [5], respectively, were included in a molecular mass calibration to estimate masses for the *P. pastoris* and *P. angusta* enzymes of 920 and 890 kDa, respectively. The FMN and iron contents of the purified enzymes were 1.0 ± 0.1 FMN and 33.2 ± 3.6 Fe per *P. pastoris* complex I, and 1.1 ± 0.2 FMN and 33.4 ± 4.5 Fe per *P. angusta* complex I, using these estimated molecular masses.

The EPR spectra of both the *P. pastoris* and *P. angusta* enzymes (see Figure 3), are typical complex I spectra, and confirm, unambiguously, the identity of the purified enzyme [35]. Comparison with the spectra from *B. taurus* complex I [35,36] is straightforward, and four signals (N1b, N2, N3 and N4) are immediately identified by their similar g-values. The N5 signal, observed in complex I from *B. taurus* and *Y. lipolytica* [33], and the N1a signal, observed in complex I from *E. coli* [37], are not observed. The slowly relaxing N2 spectrum, assigned to the [4Fe-4S] cluster in NUKM (PSST)[1], is evident at around 12 K, with g_z-values matching those from the *B. taurus* and *Y. lipolytica* enzymes (g_z = 2.06 for both *P. pastoris* and *P. angusta*). At 40 K the N1b spectrum, from the [2Fe-2S] cluster in NUAM (75 kDa), is observed, again with g_z-values matching those from *B. taurus* and *Y. lipolytica* complex I (g_z = 2.03 for both *P. pastoris* and *P angusta*). At lower temperatures (most clearly 7 and 9 K) two further [4Fe-4S] spectra are observed. The g_x value for N3, assigned to the [4Fe-4S] cluster in NUBM (51

[1] We name the subunits according to their SwissProt codes, and present the names for the *B. taurus* homologues alongside where appropriate.

kDa), is 1.86 for both *P. pastoris and P. angusta* (the g_z signal cannot be distinguished). The origin of N4 is controversial [38,39] but the g_z and g_x signals of 2.11 and 1.89 (in both cases) match closely to those from *Y. lipolytica* and *B. taurus* complex I.

Catalytic activities of the purified enzymes

Table 2 summarises the catalytic properties of the complexes I from *P. pastoris and P. angusta*, and compares them with those from *Y. lipolytica* and *B. taurus* (measured in this study). All the rates of NADH:HAR oxidoreduction are similar, but the rates of NADH:FeCN oxidoreduction are significantly higher for the two *Pichia* enzymes. Note that our reported values refer to only a single condition, so they are only an indication of the relative catalytic activities of the enzymes, and do not allow the cause of the variation to be identified. Using the structure of the hydrophilic domain of *T. thermophilus* complex I as a template, sequence comparisons for the protein around the NADH binding site in *B. taurus, Y. lipolytica, and P. angusta* have not provided any insight. The rates of NADH:DQ oxidoreduction are similar in all cases, except for the *P. pastoris* enzyme, which displays a markedly higher rate. Note that the highest published values for *Y. lipolytica* (6–7 μmol min^{-1} mg^{-1} [40]) exceed those achieved here, but are comparable to our values from *P. pastoris*. Interestingly, all four enzymes are close to completely inhibited by 2 μM piericidin A, but the three yeast enzymes are much less effectively inhibited by rotenone than the *B. taurus* enzyme (see below).

The markedly more active *P. pastoris* complex I could be reconstituted into liposomes, using methods based on those for *Y. lipolytica* [21] (see Experimental Methods), to provide well coupled proteoliposomes, typically with respiratory control ratios (RCR, the ratio of the rates of NADH oxidation in the presence and absence of an uncoupler) of ~2. Proteoliposomes formed from the less active *P. angusta* enzyme did not show any coupling (RCR = 1). Figure 4 shows typical traces monitoring the fluorescence of ACMA, a measure of ΔpH across the liposomal membrane [41], for reconstituted *P. pastoris* complex I. In the presence of valinomycin (so that potassium ion transport collapses $\Delta\psi$ and facilitates ΔpH formation) the ACMA fluorescence is rapidly quenched when catalysis is initiated. It is re-established upon the addition of a proton ionophore, FCCP, to dissipate the proton motive force, or an inhibitor (piericidin A) to prevent further proton translocation. The results shown in Figure 4 are strong evidence for proton translocation by complex I from *P. pastoris*.

Rates of reactive oxygen species (ROS) generation by the complexes I from both *Pichia* species were measured as H_2O_2 (detected using Amplex Red) or superoxide (detected using acetylated cytochrome *c*), and verified by comparison with independent measurements of the rates of NADH oxidation (see Table 2). Within experimental error, the rates of NADH oxidation matched the rates of H_2O_2 production in a 1:1 ratio, validating both measurements. In both cases, the rates of superoxide formation (one electron) are close to twice the rates of H_2O_2 formation (two electrons), indicating that the enzymes from *P. pastoris* and *P. angusta*, like the enzyme from *B. taurus* [23], produce ROS predominantly as superoxide. Table 2 shows that complex I from *Y. lipolytica* falls into the same class, although the rate of superoxide production measured here (90 nmol min^{-1} mg^{-1}, validated using the rate of NADH oxidation) is significantly higher than reported previously (18 nmoles min^{-1} mg^{-1} [42]). The cause of this discrepancy is not clear. Table 2 shows that the three yeast complexes I produce significantly more ROS than the *B. taurus* enzyme.

The protein composition of the complexes I from *P. pastoris* and *P. angusta*

Figure 5 shows an SDS PAGE analysis of the protein composition of the complexes I from *B. taurus, Y. lipolytica, P. pastoris* and *P. angusta*. The overall similarity of the pattern, particularly for the high molecular weight subunits, is striking, though differences in mass and/or migration become apparent lower down the gel. Bands corresponding to the NUAM (75 kDa), NUBM (51 kDa), NUCM (49 kDa),

NUDM/NUEM (42/39 kDa) and NUGM (30 kDa) subunits are clearly visible in all cases (NUBM and NUCM comigrate in *Y. lipolytica*), but one of the bands present in the mammalian enzyme, probably the 42 kDa subunit, does not appear in the lanes from the three yeast species.

The complexes I from *B. taurus* and *Y. lipolytica* have already been characterized extensively, using publically available sequence data, but there is little available for *P. pastoris* and *P. angusta*. In order to identify as many subunits as possible in the two *Pichia* complexes, all the visible protein bands were excised from the gels, digested with trypsin, and subjected to MALDI-TOF and tandem MS analysis. For both *P. pastoris* and *P. angusta* the observed peptide masses (from MALDI-TOF MS) were searched (for matches within 70 ppm) against the NCBI non-redundant sequence database, and against an in-house database of expected complex I subunits from *P. angusta* (derived from the NCBI genome survey sequences by comparison with known sequences from other species). Then, the closest matches to the tandem MS data (within 120 ppm) were re-evaluated using error tolerance searches, allowing for modifications and amino acid substitutions between species. A summary of the data assigned is presented in Supplementary Table S1. All seven hydrophilic core subunits, and two supernumerary subunits, were identified in the enzyme from *P. pastoris*. Six of the hydrophilic core subunits (the exception being NUKM (PSST)), and nine supernumerary subunits were identified in the enzyme from *P. angusta*. The subunits of *P. pastoris* complex I were identified using the similarity of observed peptide masses to predicted peptide masses from other fungal species, including *P. stipitis* (NUAM (75 kDa), NUBM (51 kDa), NUCM (49 kDa), NUEM (39 kDa), NUGM (30 kDa), NUHM (24 kDa), NUYM (18 kDa), NUIM (TYKY) and NUKM (PSST)), *Lodderomyces elongisporus* (NUAM), *Debaryomyces hansenii* (NUBM, NUCM, and NUHM), *Y. lipolytica* (NUBM, NUCM, and NUIM), *P. guilleromondii* (NUEM), *N. crassa* (NUKM), *Aspergillus fumigatus* (NUKM), and *Candida albicans* (NUYM). These matches confirm that *P. pastoris* complex I contains a number of canonical complex I subunits, but the lack of complete sequences for them precludes further discussion about its subunit composition and homology to other species. The genome sequence for *P. pastoris* is available commercially, and the composition of its complex I will be described in detail in a future publication. In the same way, masses from five subunits in *P. angusta* complex I were found to be similar to those in other species: *P. stipitis* (NUAM (75 kDa), and NUCM (49 kDa)), *N. crassa* (NUBM (51 kDa)), *D. hansenii* (NUCM) *Dekkera bruxellensis* (NUHM (24 kDa)), *Magnaporthe grisea* (NUHM), and *A. niger* (NB6M (B16.6)). For *P. angusta* there are several full or partial sequences available publically as genome survey sequences, and they allowed the identification of eleven complex I subunit sequences (NUBM (51 kDa), NUGM (30 kDa), NUIM (TYKY), NUZM, NIAM (ASHI), N7BM (B17.2), NUKM (B14.7), NUFM (B13), NUMM (13 kDa), NIMM (MWFE) and NIDM (PDSW)). A comparison of observed peptide masses from *P. pastoris* against these *P. angusta* sequences only provided a match to one complex I subunit (NUIM (TYKY)).

Discussion

The presence of complex I in *Pichia* species

The data presented here show that both *P. pastoris* and *P. angusta* assemble a piericidin A sensitive, multisubunit NADH:ubiquinone oxidoreductase in their mitochondria, with closely similar catalytic and spectroscopic properties to the enzymes from *B. taurus* and *Y. lipolytica*. A number of the core subunits of complex I have been identified in both *Pichia* species, along with several supernumerary subunits, which vary between kingdoms, subkingdoms and between genera and species also [7]. Our data and preliminary sequence comparisons suggest that, within the species included in Figure 1,

complex I from *P. pastoris* is most closely related to the enzyme from *P. stipitis*, whereas *P. angusta* complex I is most closely related to the enzymes from *Y. lipolytica*, *L. elongisporus*, *P. stipitis*, *P. guilleromondii* and *D. hansenii* (but not to any one of them in particular).

The presence of the complex I ND genes in the mitochondrial genomes of many fungi (including *Pichia* species) [13,28], suggests that most (if not all) obligate aerobic fungi are able to express complex I. Those species capable of facultative anaerobic fermentation encode only the single subunit enzyme (see Figure 1). Without a larger set of sequences for comparison, it is difficult to speculate further on the evolutionary development of complex I in some species, and its loss in others. However, intriguing correlations can be identified within the species in Figure 1. Only species that encode complex I encode the alternative, single subunit, non-proton pumping ubiquinol oxidase [28]: if complexes III and IV are substituted by the alternative oxidase, complex I is retained in order to maintain the proton motive force (or vice versa). Only species in the subphylum pezizomycota encode the complex I supernumerary subunit NURM [28], and they are the only species that encode the three subunit, proton pumping transhydrogenase also. In *N. crassa* NURM is a 17.8 kDa protein containing one transmembrane helix, with no known homology to any other protein.

The catalytic activities of the complexes I from *Pichia* species

The preparation of a highly pure eukaryotic complex I with native NADH:ubiquinone oxidoreductase activity has proved challenging, particularly for the mammalian complexes. Recently, by including phospholipids in the preparation, highly pure complex I has been prepared from *B. taurus* mitochondria with NADH:DQ oxidoreductase activity up to 4 μmol NADH min^{-1} mg^{-1} [22]. For *Y. lipolytica*, preparations with an activity of ~2.8 μmol min^{-1} mg^{-1} were obtained by conventional purification [33], but a histidine tag on the NUGM (30 kDa) subunit increased the activity to 6 - 7 μmol min^{-1} mg^{-1} [40]. Here, conventional methods were used to purify the two *Pichia* complexes I. Initially, it was hoped that the *P. angusta* enzyme would be more stable because of the organism's thermotolerance [18], but the *P. pastoris* enzyme gave a significantly higher activity than that of *P. angusta* (6.3 and 4.0 μmol NADH min^{-1} mg^{-1}, respectively). It is possible that phospholipid content is key to understanding the relative activities. The *B. taurus* enzyme is readily depleted of phospholipids during preparation [22]. The *P. angusta* enzyme requires more exogenous phospholipids in activity assays than the *P. pastoris* enzyme, to attain its highest activity, and it cannot be incorporated properly into liposomes. It is possible that this stems from its lower relative abundance in the membranes – it must be washed more extensively on the anion exchange column, a procedure which is known to 'strip' the *B. taurus* enzyme [22]. Finally, variations in the DQ reductase activity are not reflected in any other activity measurements (see Table 2); in particular, NADH:HAR oxidoreduction is essentially the same in all four cases. Previously, a study of the complexes I from *B. taurus* and *P. denitrificans* also found that, while FeCN was reduced relatively slowly by the prokaryotic enzyme, the HAR reduction rates were similar [43].

'Tests' which distinguish complex I from other NADH dehydrogenases, and inhibitor sensitivity

It is widely assumed that dNADH reacts only with complex I, not with alternative NADH dehydrogenases, although this fact has only been demonstrated in *E. coli* [29]. All the complexes I tested here (Table 2) react at comparable rates with dNADH and NADH. However, if the dNADH:HAR and dNADH:DQ oxidoreductase activities in the membranes are only from complex I, then the ratio between them should be conserved throughout the preparation. In fact, the ratio (HAR / DQ) increases from 1.1 (*P. pastoris*) and 5.0 (*P. angusta*) in the membranes to 9.8 and 21.1, respectively. Because the specific dNADH:HAR oxidoreductase activity is unlikely to vary significantly, the results indicate at least one additional enzyme in the membrane preparations catalyses

dNADH:DQ oxidoreduction also (or a significant portion of the dNADH:DQ activity has been lost). Consequently, dNADH may differentiate less clearly between complex I and alternative NADH dehydrogenases than commonly supposed. It is widely assumed that only complex I catalyses NADH:HAR oxidoreduction also (see, for example [11]) but we have been unable to find any published data to support this fact. During the preparation of *P. angusta* complex I, two fractions with NADH:HAR oxidoreductase activity eluted from the anion exchange column, but only the second catalysed dNADH:DQ oxidoreduction. Although the protein composition of the first peak was complex, SDS PAGE, mass spectrometry and Western blotting analyses detected no evidence for complex I or any portion it, suggesting that this second 'test' for complex I is also not definitive.

Table 2 shows that all the NADH:DQ oxidoreductase activities tested are strongly inhibited by piericidin A, but rotenone does not inhibit the three yeast enzymes as strongly as the *B. taurus* enzyme. This observation may explain why rotenone-sensitive NADH oxidation was not observed previously in *P. pastoris* mitochondria [14]. Studies of the inhibition of the activity of *P. pastoris* complex I over a range of rotenone concentrations showed that almost complete inhibition can be observed, but only at much higher concentrations (~96% in 50 μM rotenone). Relatively weak inhibition of *Y. lipolytica* complex I was observed previously also [42]. Thus, rotenone is regarded as an archetypal complex I inhibitor simply because of the predominance of the *B. taurus* enzyme in early studies.

The production of reactive oxygen species

Previously, we described a mechanism for ROS production by the reduced flavin in complex I from *B. taurus*, and demonstrated the same mechanism in complex I from *E. coli* [23,44]. Here, we compare ROS production by the complexes I from *P. pastoris*, *P. angusta* and *Y. lipolytica* with that by the *B. taurus* enzyme. Values for all three yeast species were significantly higher than those from *B. taurus*, and those for the two *Pichia* species were the highest. This is particularly interesting because *B. taurus* and *E. coli* complex I exhibit similar rates [44]. When the two *Pichia* species are grown on methanol the induction of alcohol oxidases results in significant H_2O_2 production, which is metabolised by catalase and cytochrome *c* peroxidase [17,45]. The additional contribution from complex I may not be significant in this context. Furthermore, all four eukaryotic enzymes produce predominantly superoxide, not H_2O_2. This observation maintains the correlation between superoxide to H_2O_2 ratio and the reduction of cluster N1a described previously [44]: the N1a EPR signal from the [2Fe-2S] cluster in NUHM (24 kDa) is not observed in any of the eukaryotic enzymes described here (see Figure 3). Therefore, the cluster is predominantly oxidized in the presence of NADH, and is, in principle, available to transiently accept the second electron from the fully reduced flavin, promoting the escape of nascent superoxide from the active site.

Acknowledgements

We thank Professor Ulrich Brandt (Frankfurt) for providing the strain of *Y. lipolytica*, Dr. Ian M. Fearnley (MRC) for advice on mass spectrometry, and Martin King (MRC) for providing *B. taurus* complex I. This work was supported by The Medical Research Council.

References

1. Brandt, U. (2006) Energy converting NADH:quinone oxidoreductase (complex I). Annu. Rev. Biochem. **75**, 69-92
2. Hirst, J. (2005) Energy transduction by respiratory complex I - an evaluation of current knowledge. Biochem. Soc. Trans. **33**, 525-529
3. Sazanov, L. A., and Hinchliffe, P. (2006) Structure of the hydrophilic domain of respiratory complex I from *Thermus thermophilus*. Science **311**, 1430-1436
4. Hirst, J., Carroll, J., Fearnley, I. M., Shannon, R. J., and Walker, J. E. (2003) The nuclear encoded subunits of complex I from bovine heart mitochondria. Biochim. Biophys. Acta **1604**, 135-150
5. Morgner, N., Zickermann, V., Kerscher, S., Wittig, I., Abdrakhmanova, A., Barth, H.-D., Brutschy, B., and Brandt, U. (2008) Subunit mass fingerprinting of mitochondrial complex I. Biochim. Biophys. Acta **1777**, 1384-1391
6. Marques, I., Duarte, M., Assunção, J., Ushakova, A. V., and Videira, A. (2005) Composition of complex I from *Neurospora crassa* and disruption of two accessory subunits. Biochim. Biophys. Acta **1707**, 211-220
7. Gabaldón, T., Rainey, D., and Huynen, M. A. (2005) Tracing the evolution of a large protein complex in the eukaryotes, NADH:ubiquinone oxidoreductase (complex I). J. Mol. Biol. **348**, 857-870
8. DiMauro, S., and Schon, E. A. (2003) Mitochondrial respiratory-chain diseases. New Engl. J. Med. **348**, 2656-2668
9. Greenamyre, J. T., and Hastings, T. G. (2004) Parkinson's - divergent causes, convergent mechanisms. Science **304**, 1120-1122
10. Videira, A. (1998) Complex I from the fungus *Neurospora crassa*. Biochim. Biophys. Acta **1364**, 89-100
11. Kerscher, S., Dröse, S., Zwicker, K., Zickermann, V., and Brandt, U. (2002) *Yarrowia lipolytica*, a yeast genetic system to study mitochondrial complex I. Biochim. Biophys. Acta **1555**, 83-91
12. Kriventseva, E. V., Rahman, N., Espinosa, O., and Zdobnov, E. M. (2008) OrthoDB: the hierarchical catalog of eukaryotic orthologs. Nucleic Acids Res. **36**, D271-D275
13. Nosek, J., and Fukuhara, H. (1994) NADH dehydrogenase subunit genes in the mitochondrial DNA of yeasts. J. Bacteriol. **176**, 5622-5630
14. González-Barroso, M. M., Ledesma, A., Lepper, S., Pérez-Magán, E., Zaragoza, P., and Rial, E. (2006) Isolation and bioenergetic characterization of mitochondria from *Pichia pastoris*. Yeast **23**, 307-313
15. Ruiz-Herrera, J., and Sentandreu, R. (2002) Different effectors of dimorphism in *Yarrowia lipolytica*. Arch. Microbiol. **178**, 477-483
16. Morín, M., Monteoliva, L., Insenser, M., Gil, C., and Domínguez, A. (2007) Proteomic analysis reveals metabolic changes during yeast to hypha transition in *Yarrowia lipolytica*. J. Mass Spectrom. **42**, 1453-1462
17. Gellissen, G., Kunze, G., Gaillardin, C., Cregg, J. M., Berardi, E., Veenhuis, M., and van der Klei, I. (2005) New yeast expression platforms based on methylotrophic *Hansenula polymorpha* and *Pichia pastoris* and on dimorphic *Arxula adeninivorans* and *Yarrowia lipolytica* - a comparison. FEMS Yeast Res. **5**, 1079-1096
18. van Uden, N., Abranches, P., and Cabeça-Silva, C. (1968) Temperature functions of thermal death in yeasts and their relation to the maximum temperature for growth. Arch. Mikrobiol. **61**, 381-393

19. Kerscher, S. J., Okun, J. G., and Brandt, U. (1999) A single external enzynme confers alternative NADH:ubiqinone oxidoreductase activity in *Yarrowia lipolytica*. J. Cell Sci. **112**, 2347-2354
20. Kashani-Poor, N., Kerscher, S., Zickermann, V., and Brandt, U. (2001) Efficient large scale purification of his-tagged proton translocating NADH:ubiquinone oxidoreductase (complex I) from the strictly aerobic yeast *Yarrowia lipolytica*. Biochim. Biophys. Acta **1504**, 363-370
21. Dröse, S., Galkin, A., and Brandt, U. (2005) Proton pumping by complex I from *Yarrowia lipolytica* reconstituted into proteoliposomes. Biochim. Biophys. Acta **1710**, 87-95
22. Sharpley, M. S., Shannon, R. J., Draghi, F., and Hirst, J. (2006) Interactions between phospholipids and NADH:ubiquinone oxidoreductase (complex I) from bovine mitochondria. Biochemistry **45**, 241-248
23. Kussmaul, L., and Hirst, J. (2006) The mechanism of superoxide production by NADH:ubiquinone oxidoreductase (complex I) from bovine heart mitochondria. Proc. Natl. Acad. Sci. USA **103**, 7607-7612
24. Burch, H. B. (1957) Fluorimetric assay of FAD, FMN and riboflavin. Methods Enzymol. **3**, 960-962
25. Pieroni, L., Khalil, L., Charlotte, F., Poynard, T., Piton, A., Hainque, B., and Imbert-Bismut, F. (2001) Comparison of bathophenanthroline sulfonate and ferene as chromogens in colorimetric measurement of low hepatic iron concentration. Clin. Chem. **47**, 2059-2061
26. Perkins, D. N., Pappin, D. J. C., Creasy, D. M., and Cottrell, J. S. (1999) Probability-based protein identification by searching sequence databases using mass spectrometry data. Electrophoresis **20**, 3551 - 3567
27. Melo, A. M. P., Bandeiras, T. M., and Teixeira, M. (2004) New insights into type II NAD(P)H: quinone oxidoreductases. Microbiol. Mol. Biol. R. **68**, 603-616
28. Lavín, J. L., Oguiza, J. A., Ramírez, L., and Pisabarro, A. G. (2008) Comparative genomics of the oxidative phosphorylation system in fungi. Fungal Genet. Biol. **45**, 1248-1256
29. Matsushita, K., Ohnishi, T., and Kaback, H. R. (1987) NADH-ubiquinone oxidoreductases of the *Escherichia coli* aerobic respiratory chain. Biochemistry **26**, 7732-7737
30. Katz, R., Kilpatrick, L., and Chance, B. (1971) Aquisition and loss of rotenone sensitivity in *Torulopsis utilis*. Eur. J. Biochem. **21**, 301-307
31. Grossman, S., Cobley, J. G., Singer, T. P., and Beinert, H. (1974) Reduced nicotinamide adenine dinucleotide dehydrogenase, piericidin sensitivity, and site 1 phosphorylation in different growth phases of *Candida utilis*. J. Biol. Chem. **249**, 3819-3826
32. Schwitzguébel, J.-P., and Palmer, J. M. (1982) Properties of mitochondria as a function of the growth stages of *Neurospora crassa*. J. Bacteriol. **149**, 612-619
33. Djafarzadeh, R., Kerscher, S., Zwicker, K., Radermacher, M., Lindahl, M., Schägger, H., and Brandt, U. (2000) Biophysical and structural characterization of proton-translocating NADH-dehydrogenase (complex I) from the strictly aerobic yeast *Yarrowia lipolytica*. Biochim. Biophys. Acta **1459**, 230-238
34. Carroll, J. Fearnley, I. M., Skehel, J. M., Shannon, R. J., Hirst, J., and Walker, J. E. (2006) Bovine complex I is a complex of forty-five different subunits. J. Biol. Chem. **281**, 32724-32727
35. Ohnishi, T. (1998) Iron-sulphur clusters/semiquinones in complex I. Biochim. Biophys. Acta **1364**, 186-206
36. Reda, T., Barker, C. D., and Hirst, J. (2008) Reduction of the iron-sulfur clusters in mitochondrial NADH:ubiquinone oxidoreductase (complex I) by Eu^{II}-DTPA, a very low potential reductant. Biochemistry **47**, 8885-8893

37. Uhlmann, M., and Friedrich, T. (2005) EPR signals assigned to Fe/S cluster N1c of the *Escherichia coli* NADH:ubiquinone oxidoreductase derive from cluster N1a. Biochemistry **44**, 1653-1658
38. Yakovlev, G., Reda, T., and Hirst, J. (2007) Reevaluating the relationship between EPR spectra and enzyme structure for the iron-sulfur clusters in NADH:quinone oxidoreductase. Proc. Natl. Acad. Sci. USA **104**, 12720-12725
39. Ohnishi, T., and Nakamaru-Ogiso, E. (2008) Were there any misassignments among iron-sulfur clusters N4, N5 and N6b in NADH-quinone oxidoreductase (complex I). Biochim. Biophys. Acta **1777**, 703-710
40. Dröse, S., Zwicker, K., and Brandt, U. (2002) Full recovery of the NADH:ubiquinone activity of complex I (NADH:ubiquinone oxidoreductase) from *Yarrowia lipolytica* by the addition of phospholipids. Biochim. Biophys. Acta **1556**, 65-72
41. Dufour, J.-P., Goffeau, A., and Tsong, T. Y. (1982) Active proton uptake in lipid vesicles reconstituted with the purified yeast plasma membrane ATPase. J. Biol. Chem. **257**, 9365-9371
42. Galkin, A., and Brandt, U. (2005) Superoxide radical formation by pure complex I (NADH:ubiquinone oxidoreductase) from *Yarrowia lipolytica*. J. Biol. Chem. **280**, 30129-30135
43. Zickermann, V., Kurki, S., Kervinen, M., Hassinen, I., and Finel, M. (2000) The NADH oxidation domain of complex I: do bacterial and mitochondrial enzymes catalyze ferricyanide reduction similarly ? Biochim. Biophys. Acta **1459**, 61-68
44. Esterházy, D., King, M. S., Yakovlev, G., and Hirst, J. (2008) Production of reactive oxygen species by complex I (NADH:ubiquinone oxidoreductase) from *Escherichia coli* and comparison to the enzyme from mitochondria. Biochemistry **47**, 3964-3971
45. Duff, S. J. B., and Murray, W. D. (1990) Metabolism of hydrogen peroxide by *Pichia pastoris*. Agric. Biol. Chem. **54**, 1967-1973

Tables

Table 1. Specific activities of the mitochondrial membranes from *P. pastoris* and *P. angusta*.

	Catalytic activity (μmol NADH min^{-1} mg^{-1})	
	P. pastoris	*P. angusta*
NADH:FeCN oxidoreduction	9.39 ± 0.56	9.65 ± 1.02
dNADH:FeCN oxidoreduction	6.85 ± 0.18	6.88 ± 0.88
NADH:HAR oxidoreduction	1.00 ± 0.07	1.41 ± 0.18
dNADH:HAR oxidoreduction	1.14 ± 0.07	1.34 ± 0.14
NADH:DQ oxidoreduction	1.27 ± 0.07	2.16 ± 0.40
dNADH:DQ oxidoreduction	1.00 ± 0.07	0.27 ± 0.14
NADH:DQ oxidoreduction + piericidin A	0.19 ± 0.06 (85%)	1.63 ± 0.31 (25%)
dNADH:DQ oxidoreduction + piericidin A	0.10 ± 0.04 (90%)	0.10 ± 0.01 (63%)
NADH:DQ oxidoreduction + rotenone	0.95 ± 0.52 (26%)	1.71 ± 0.40 (21%)
dNADH:DQ oxidoreduction + rotenone	0.28 ± 0.03 (72%)	0.12 ± 0.02 (56%)
Accessibility of NADH binding sites	86.2 ± 1.8 %	87.1 ± 8.3 %

Conditions: 20 mM Tris-HCl pH 7.5, 100 μM NADH or dNADH, 100 μM DQ, 3.5 mM HAR, 2 mM FeCN, 5 μM rotenone, 2 μM piericidin A, 32 °C. The accessibility of the NADH binding sites in the two preparations was determined from the average increase in the rates of dNADH:HAR, dNADH:FeCN and NADH:FeCN oxidoreduction, following solubilisation of the membranes in 3% DDM.

Table 2. Specific activities of the complexes I purified from *P. pastoris* and *P. angusta*, and comparison with the enzymes from *Y. lipolytica* and *B. taurus*.

	Catalytic activity (μmol NADH min^{-1} mg^{-1})			
	P. pastoris	*P. angusta*	*Y. lipolytica*	*B. taurus*
NADH:FeCN oxidoreduction	302.6 ± 22.9	248.9 ± 22.9	140.8 ± 3.1	111.1 ± 8.3
NADH:HAR oxidoreduction	70.5 ± 9.4	63.4 ± 3.2	68.8 ± 13	72.5 ± 6.8
dNADH:HAR oxidoreduction	68.6 ± 7.4	69.0 ± 5.3	-	-
NADH:DQ oxidoreduction	6.27 ± 0.38	4.00 ± 0.04	3.80 ± 0.55	3.82 ± 0.17
dNADH:DQ oxidoreduction	7.00 ± 0.86	3.27 ± 0.26	3.55 ± 0.40	3.62 ± 0.50
dNADH:DQ oxidoreduction + piericidin A	0.37 ± 0.30 (95%)	0.06 ± 0.01 (98%)	0.28 ± 0.02 (92%)	0.24 ± 0.11 (93%)
dNADH:DQ oxidoreduction + rotenone	2.02 ± 0.53 (71%)	0.56 ± 0.11 (83%)	1.31 ± 0.67 (63%)	0.14 ± 0.01 (96%)
	H_2O_2 or superoxide production (nmol min^{-1} mg^{-1})			
H_2O_2	63.3 ± 4.9	76.3 ± 14.7	42.5 ± 4.4	23.6 ± 5.6
superoxide	105.0 ± 11.6	127.2 ± 7.5	90.3 ± 2.8	41.3 ± 1.8
NADH:O_2 oxidoreduction	55.1 ± 5.8	68.6 ± 15.6	41.3 ± 1.8	20.1 ± 1.7

Conditions: 20 mM Tris-HCl pH 7.5, 100 μM NADH, 100 μM DQ, 3.5 mM HAR, 2 mM FeCN, 5 μM rotenone, 2 μM piericidin A, 32 °C. H_2O_2 measurements: 20 mM Tris-HCl pH 7.5, 30 μM NADH, 10 μM Amplex Red, 2 U ml^{-1} horse radish peroxidase. Superoxide measurements: 20 mM Tris-HCl pH 7.5, 30 μM NADH, 50 μM partially acetylated cytochrome *c*. Values for *Y. lipolytica* and *B. taurus* were measured alongside those for *P. pastoris* and *P. angusta* for direct comparison.

Figure legends

Figure 1. Phylogenetic tree showing the distribution of complex I within the subkingdom of dikarya. Species in **bold** have complex I subunits encoded in their nuclear and mitochondrial genomes, and they encode an alternative oxidase and at least one alternative, single subunit NADH:ubiquinone oxidoreductase. Species in grey are able to anaerobically ferment, and they only encode alternative NADH:ubiquinone oxidoreductases. (*) denotes the presence of the genes for the three subunit mitochondrial transhydrogenase, and the NURM gene, which has been observed previously only in *N. crassa* complex I. The phylogenetic tree was adapted from [12].

Figure 2. Variation of the specific dNADH:HAR oxidoreductase activity during preparation of the complexes I from *P. pastoris* and *P. angusta*. Memb., mitochondrial membranes; Sol. Memb., membranes following solubilization in DDM; QS, pooled fractions from the Q-sepharose ion exchange chromatography step; SE2, pooled fractions from the second size exclusion chromatography step.

Figure 3. EPR spectra showing signals from the FeS clusters in the complexes I from *P. pastoris* and *P. angusta* reduced by NADH. Spectra are presented at different temperatures because each cluster signal is only observed over a limited range. The signals have been identified, and labeled, by matching their g-values and temperature dependence to those from the well characterized complexes I from *B. taurus* and *Y. lipolytica*. Conditions: ~15 mg mL^{-1} complex I, 5 mM NADH, 20 mM MOPS pH 7.5, 150 mM NaCl and 0.02% DDM; microwave power 1 mW, conversion time 81.92 ms, time constant 20.48 ms, modulation amplitude 10 G, microwave frequency ~9.38 MHz.

Figure 4. Proton pumping by complex I from *P. pastoris* reconstituted into liposomes. The formation of ΔpH was monitored by the fluorescence of ACMA, which is quenched upon accumulation into the lumen of the liposomes. A small decrease in fluorescence, not related to the formation of ΔpH, is observed upon the addition of DQ. Significant quenching (ΔpH formation) is observed in the presence of both NADH and DQ, and is dissipated by the presence of either the proton ionophore FCCP, or the complex I inhibitor piericidin A. The potassium ionophore, valinomycin, is present to collapse $\Delta\psi$ and allow ΔpH formation. The traces all begin at zero fluorescence intensity and have been offset from one another along the y-axis. Conditions: 100 μM NADH, 100 μM DQ, 500 nM ACMA, 5 μM valinomycin, 20 mM MOPS pH 7.5 and 50 mM KCl, excitation 430 nm, emission 475 nm.

Figure 5. Analysis of the subunit composition of the complexes I from *P. pastoris* and *P. angusta*, and comparison with the enzymes from *B. taurus* and *Y. lipolytica*. SDS-PAGE analysis was performed on a 12 - 22% gradient gel, and the bands excised and analyzed by peptide mass fingerprinting and tandem mass spectrometry. Peptides were identified using publicly available genome sequences (see Supplementary Table S1).

Figure 1

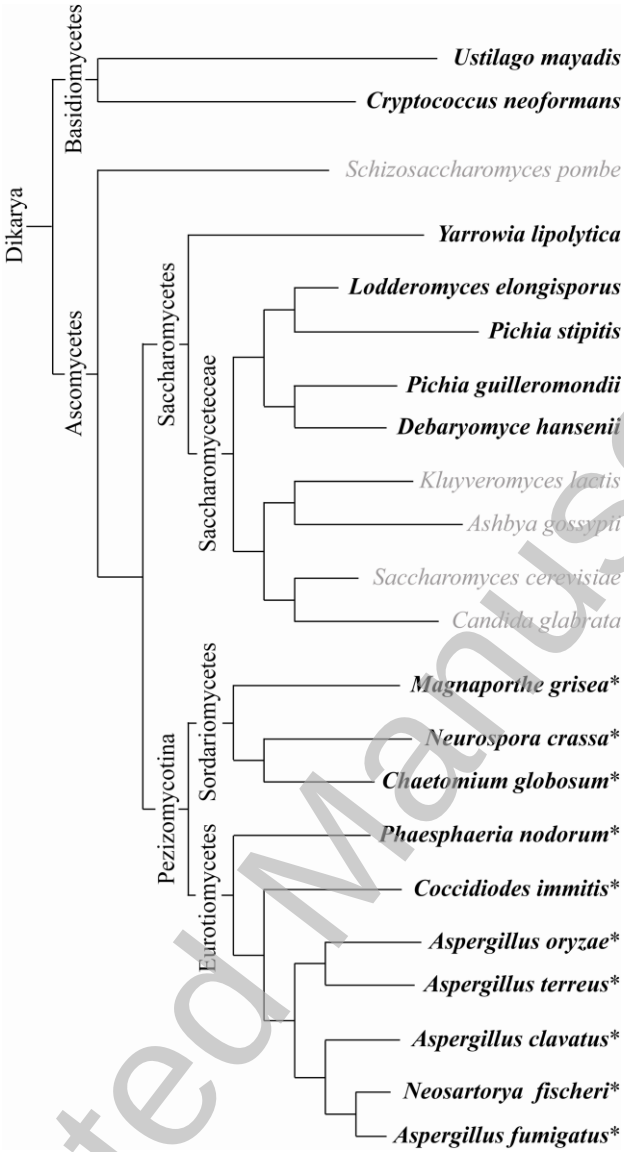

Figure 2

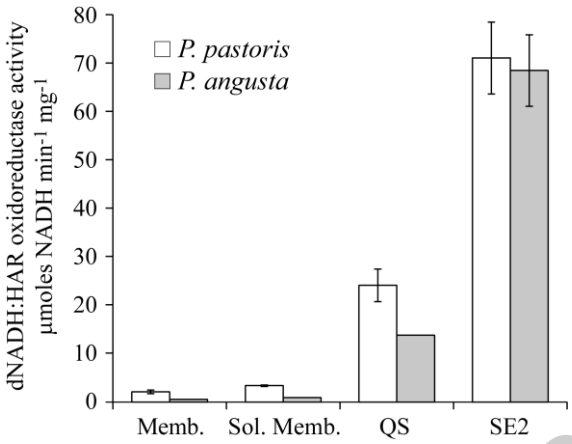

Figure 3

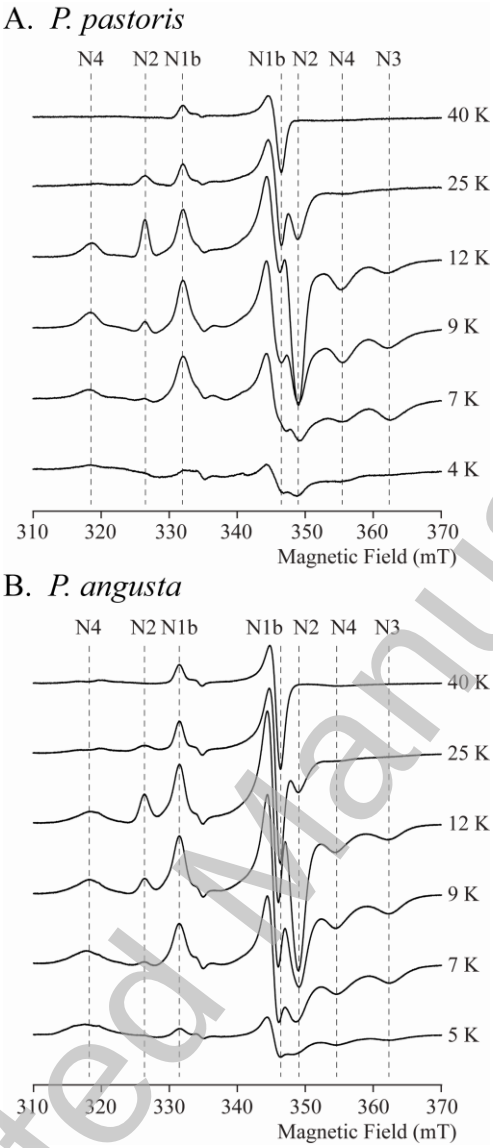

Figure 4

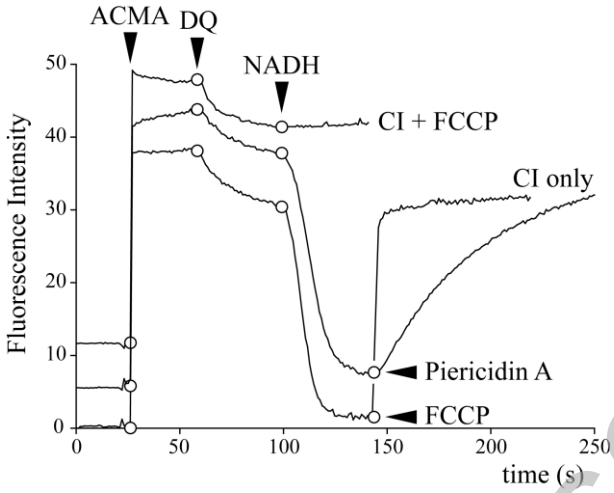

Figure 5